Towards Reducing the Number of Crashes during Hurricane Evacuation: Assessing the Potential Safety Impact of Adaptive Cruise Control Systems

Rezaur Rahman
Ph.D. Student
Department of Civil, Environmental, and Construction Engineering
University of Central Florida
12800 Pegasus Drive, Orlando, FL 32816
Phone: 321-946-3184
Email: rezaur.rahman@knights.ucf.edu

Samiul Hasan, Ph.D.
(Corresponding Author)
Assistant Professor
Department of Civil, Environmental, and Construction Engineering
University of Central Florida
12800 Pegasus Drive, Orlando, FL 32816
Phone: 407-823-2480
Email: samiul.hasan@ucf.edu

Mohamed H. Zaki, Ph.D.
Assistant Professor
Department of Civil, Environmental, and Construction Engineering
University of Central Florida
12800 Pegasus Drive, Orlando, FL 32816
Phone: 407-823-4824
Email: mzaki@ucf.edu

[This is the pre-print version of the following article: Rahman, Hasan, and Zaki (2021). Towards Reducing the Number of Crashes during Hurricane Evacuation: Assessing the Potential Safety Impact of Adaptive Cruise Control Systems. Transportation Research Part C: Emerging Technologies, 128, 103188, which has been published in final form at https://doi.org/10.1016/j.trc.2021.103188*].*

ABSTRACT

Ensuring safer mobility for evacuee drivers during a hurricane evacuation has always been a major concern for traffic managers. That concern has grown further, particularly after recent hurricanes, which forced millions of people to evacuate, causing significant congestion and a high number of traffic crashes. Though several strategies have been deployed to manage the heavy traffic demand during a hurricane evacuation, current approaches seem to have less impact on traffic safety. In a situation where people are ordered to evacuate to a safer place involving long hours of driving, perception related errors are inevitable. In such conditions, advanced driving assistance system or vehicle automation can have a positive impact. In this study, we assess the safety impact of Adaptive Cruise Control (ACC) systems during an evacuation. We develop a microscopic simulation model of evacuation traffic in SUMO and calibrate it using real-world traffic data collected during the evacuation period of hurricane Irma for a segment in the Interstate highway in Florida. To evaluate the safety impact of ACC systems, we adopt two surrogate measures: time to collision (TTC) and deceleration rate to avoid a collision (DRAC). Our simulation experiments show that, during the evacuation, about 49.7% of traffic collisions can be reduced at a 25% market penetration of ACC equipped vehicles. Our result has potential implications for hurricane evacuation management since a modest decrease in the number of crashes can help reduce the massive delays most commonly experienced during a major evacuation.

Index Terms – Hurricane Evacuation, Stop-and-go Traffic, Microscopic Traffic Simulation, Surrogate Safety Measures, Adaptive Cruise Control.

1. Introduction

Devastating experiences from recent hurricanes such as Harvey, Irma, Maria, Florence, and Michael have made emergency evacuation a major issue for the coastal residents of the United States. For instance, during hurricane Irma in Florida, about 6.5 million residents were ordered to evacuate, which caused significant traffic congestion and delay on two major freeways (I-75 and I-95) available for leaving Florida. Evacuation creates a surge in traffic demand resulting in irregular traffic flow patterns, which may cause traffic crashes. In such critical situations, a challenge for transportation and emergency management agencies is to ensure safe and efficient evacuation of a significantly large number of people. Several strategies have been deployed to manage traffic during evacuation (Murray-Tuite et al., 2017). However, these strategies seem to be less effective in reducing the number of traffic crashes. During the evacuation period of hurricane Irma, about 221 crashes occurred on I-75 from September 6 to September 9, 2017 (before the landfall day), which also caused significant delay for the evacuees. Despite the high number of crashes, studies related to evacuation traffic modeling and safety analysis are less common and inadequate to address the severity of this problem.

During an evacuation period, the traffic stream follows oscillatory speed, similar to a stop and go wave, potentially contributing to rear-end crashes (Abdel-aty et al., 2004; Tanishita and van Wee, 2017; Wu et al., 2018). Previous studies have shown that, in a stop and go traffic condition, rear-

end collisions are the primary collision type, which occurs due to frequent acceleration and deceleration induced by the propagation of kinematic waves (Abdel-Aty and Abdelwahab, 2003; Kim et al., 2007; Li et al., 2017a). Also, the most dangerous situation occurs when the leading vehicle is forced to deaccelerate while the following vehicle maintains high speed (Abdel-Aty et al., 2005; Xu et al., 2012; Zheng et al., 2010). Ye Li et al. (Li et al., 2017a) found that rear-end collisions in stop and go traffic depends on three parameters: perception-reaction time, the initial gap between vehicles, and deceleration ability. These factors largely depend on the driver's perception of traffic conditions. In hurricane evacuation—when evacuees are eager to reach a safe destination and are frustrated due to long hours of driving through highly congested highways—perception related errors are inevitable. Thus, unstable traffic flow leading to driver's perception error may contribute to a high number of collisions during a hurricane evacuation.

To reduce the number of crashes during the evacuation, we cannot just rely on infrastructure-based solutions. We also need advanced traffic management strategies that will improve traffic stability as well as provide route guidance and assistance to the drivers to ensure safety. Strategies like contraflow to facilitate evacuation traffic or use of hard shoulder as an extra lane increase roadway capacity to manage the high volume of traffic. However, these strategies will not address and improve an evacuee's perception related errors reducing the number of crashes. In such cases, in-vehicle driving assistance systems can offer a viable solution.

In this study, we assess the safety impacts of an Adaptive Cruise Control (ACC) system during an evacuation period. ACC systems are commonly designed to maintain a constant time-gap (CTG) between vehicles when following a vehicle. Several studies have shown that the ACC system substantially reduces traffic collisions (Li et al., 2017a; Wang and Rajamani, 2004), especially rear-end crashes, under regular traffic demand. In this paper, we present a microscopic traffic simulation-based study using SUMO to evaluate the impact of the ACC system on improving traffic safety during evacuation. To develop the simulation model, we have collected traffic data for Interstate 75 (I-75) between September 3 and September 16, 2017, which includes the evacuation period of hurricane Irma. We develop and calibrate a microscopic traffic simulation model to replicate the evacuation traffic behavior. Then we add ACC equipped vehicles at different market penetration rates (MPR) to check the overall improvement in traffic collisions. Thus, this study has made two significant contributions:

(i) It calibrates, for the first time to the best of our knowledge, a microscopic traffic simulation model using real-world hurricane evacuation data and offers more in-depth insights on driver behavior during evacuations, and

(ii) It provides experimental evidence of potential safety impact of advanced driving assistance systems, for transportation agencies, during a hurricane evacuation.

2. Literature Review

In recent times, automobile industries have been experimenting new state-of-the-art technologies such as advanced collision warning (Aust et al., 2013; Bueno et al., 2014), vehicle to vehicle (V2V) and vehicle to infrastructure (V2I) communication (Harigovindan et al., 2014; Li et al., 2016; Rahman et al., 2018; Rahman and Abdel-Aty, 2018; van Nunen et al., 2012), and automated driving systems (Jeong et al., 2017; Martín de Diego et al., 2013; Zeeb et al., 2015). The definition of an automated vehicle is more generic including five levels of automation (Talebpour and Mahmassani, 2016) with each level consisting certain upgraded features associated with longitudinal and lateral control of a vehicle. Currently, fully automated vehicles are not available in the market, and they are going through rigorous regulatory scrutiny and field experiments. However, several low-level automation technologies, such as vehicle adaptive cruise control (ACC), have already been introduced and are likely to expand their market in the coming years (Bose and Ioannou, 2003; Kesting et al., 2008; Marsden et al., 2001; Tapani, 2012; Yue et al., 2018).

An adaptive cruise control system is a state-of-the-art driving assistance system that allows the vehicle to maintain a constant gap with the leading vehicle by automatically adapting to the speed variation. Several studies have evaluated the impact of ACC equipped vehicles on traffic flow and safety. Studies have claimed that ACC technologies reduce the variation of vehicle acceleration (Li et al., 2017a; Marsden et al., 2001; Tapani, 2012) and stabilize traffic (Kesting et al., 2008). While some field tests of commercially available ACC systems have shown that the strings of ACC equipped vehicles might not be stable and the speed oscillation was amplified from the initial vehicle to the following vehicles (Milanes et al., 2014; Milanés and Shladover, 2014). The impact of the ACC system largely depends on the parameter setting, but in the field experiment, the parameters are allowed to adjust only within a small range (Li et al., 2017c). In the future, the adjustability range of the parameters could be improved with the advancement in the radar detection quality, processing and communication speed, and inherent feedback controllers, which will affect the operation of vehicle strings. However, the impacts of the parameters in ACC systems on traffic operation, especially during stop and go traffic has not thoroughly evaluated.

Few studies have been conducted to assess the safety impact of the ACC system, especially for an oscillatory traffic condition. Recently, Li et al. (7) have evaluated the safety impact of ACC equipped vehicles in oscillatory traffic, which showed that ACC equipped vehicles can significantly reduce the number of crashes. However, this study has been conducted with synthetic data generated in a predefined control environment (e.g., controlling speed distribution, acceleration, headway, and demand) to replicate the congested oscillatory traffic condition. To the best of our knowledge, no study has evaluated the safety and mobility impact of these advanced technologies while dealing with a more critical situation such as a hurricane evacuation. In this study, we aim to fill this research gap by assessing the safety impact of the ACC system during hurricane evacuation using a microscopic simulation-based approach with a more realistic experimental setup and real-world evacuation data.

3. Data and Methods

3.1. Data Description and Preparation

We have collected the data for a 9.5 miles long segment of the I-75 (Fig. 1(a)) from the Regional Integrated Transportation Information System (RITIS) database, which includes traffic data from September 3 to September 17, 2017. This time span covers the evacuation period of hurricane Irma. We have observed previous evacuation patterns to understand the most critical evacuation routes. We have found that during an evacuation, a large portion of residents living in Florida evacuates to Georgia or adjacent states. Hence, we have chosen a study segment on I-75 between Ocala to Gainesville, a road segment that serves a major portion of the evacuation traffic during Irma. We extract the data from 11 microwave vehicle detectors (MVDS) (Fig. 1(b)). Among these detectors, we are unable to extract any data from three detectors. These detectors might have been dysfunctional during the evacuation period, so they could not record any traffic information. Each MVDS detector provides speed, volume, and occupancy at a high resolution (every 20 to 30 seconds).

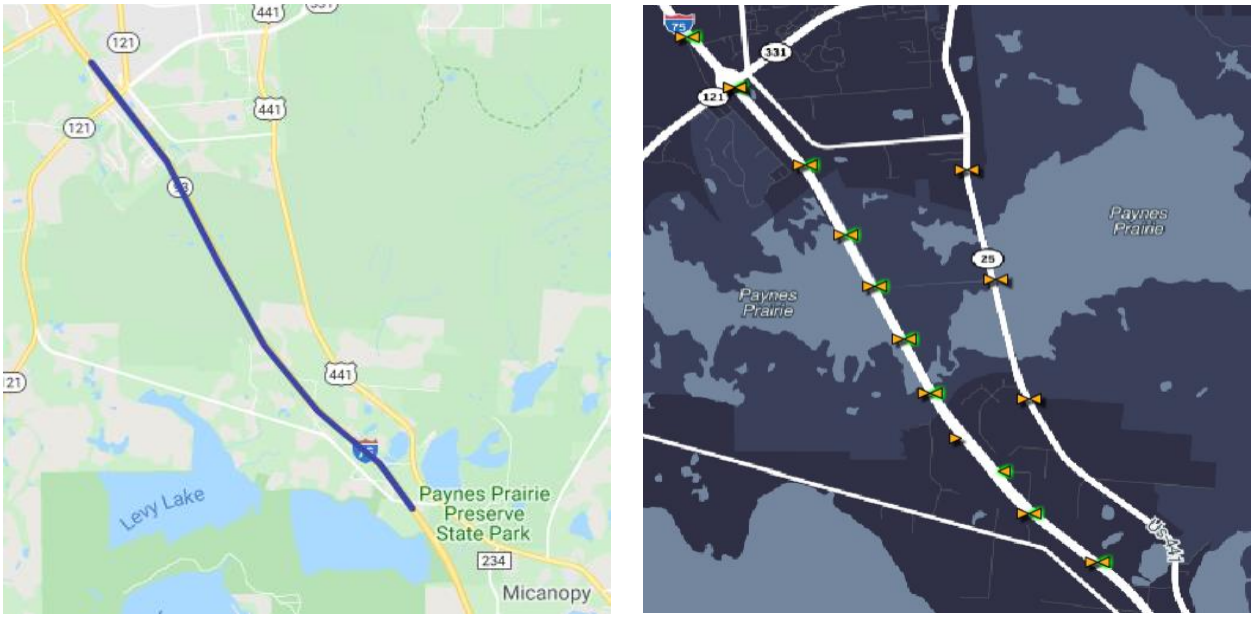

(a) (b)

Fig. 1. Study Segment on I-75: (a) Google Map View of the Route (b) Location of the MVDS detectors

Previous studies (Abdel-Aty and Wang, 2017; Katrakazas et al., 2018; Lee et al., 2016), investigating highway safety using microsimulation, aggregated input data over 5 to 15 min intervals. For evacuation traffic condition, the traffic speed variations are expected to be more abrupt within a small-time interval (Rahman and Hasan, 2018), hence we choose a 5-minute interval for aggregating the input data. While processing the data, we observe some missing values for speed and volume. We apply a simple rolling average method with a window size of three to

replace the missing values—by taking the average from the previous three available interval values.

The raw data collected from traffic detectors are subjected to errors. Several factors such as detector malfunctioning, false encoding during storing the data into the server, overlapping of multiple entries, duplicate entries, and bad weather conditions can cause errors. For example, in some cases during congested stop and go traffic conditions, microwave radar detectors fail to detect the immobile vehicles, hence provide misleading information. Therefore, before proceeding to model preparation, we need to check the outliers in the dataset. We use 1.5 times the interquartile range (IQR) as the boundary to detect the outlier inside the data. The interquartile range is the difference between the first quartile (Q_1) and third quartile (Q_3) of a data sample. Outliers are defined as observations that fall below $Q_1 - 1.5\,IQR$ or above $Q_3 + 1.5\,IQR$. From this process, we observe very few outliers. Similar to missing values, we replace the outliers using the rolling average method.

We have also collected incident data for the study area from the RITIS incident database. The incident data covers four types of incidents: crash, weather-related incident, congestion, and other regular events (disabled vehicle, road construction related delay, etc.).

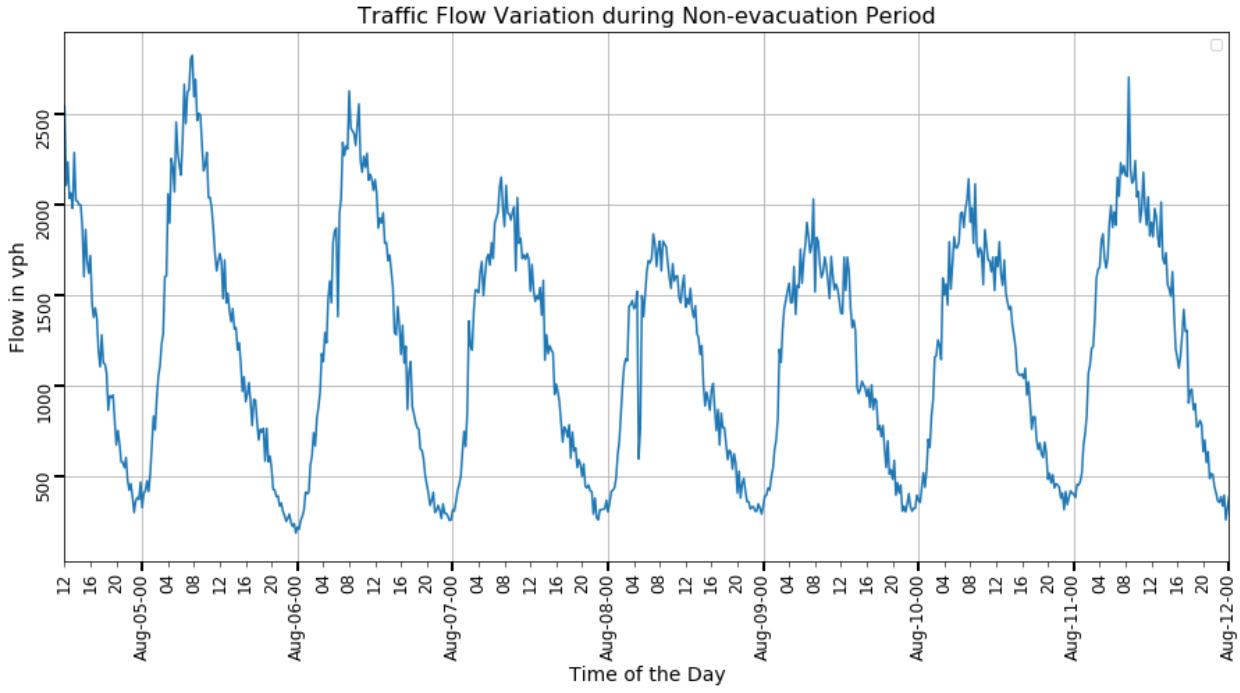

(a)

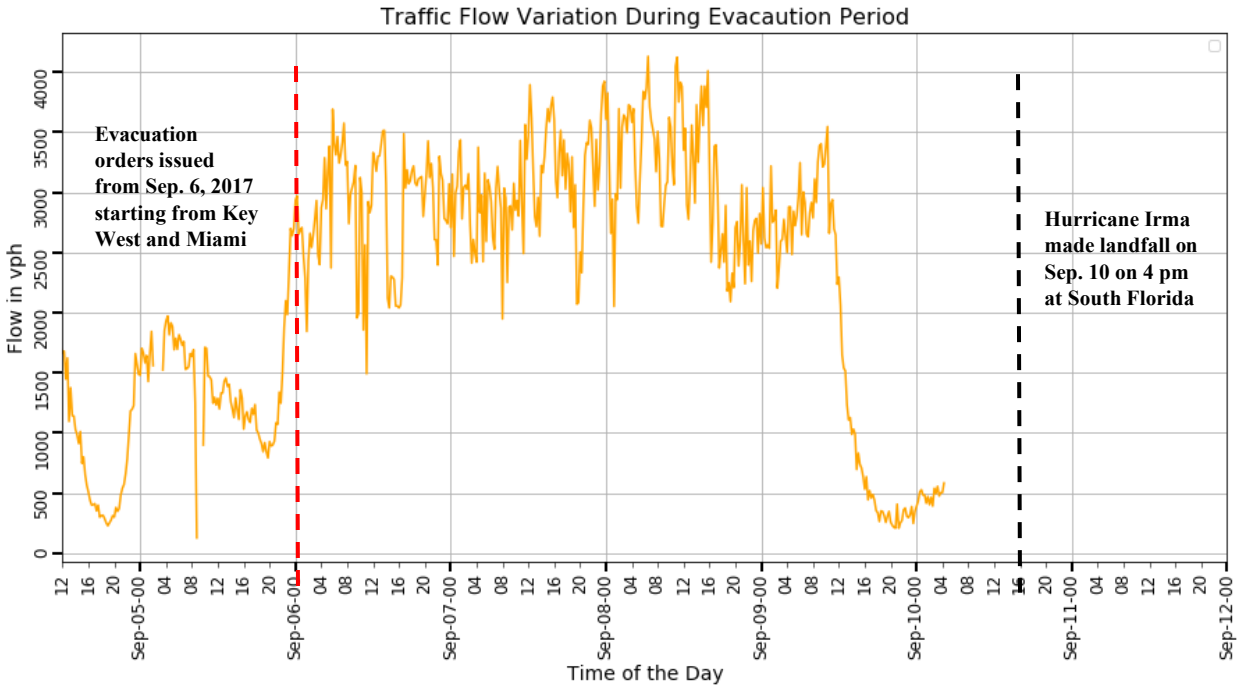

(b)

Fig. 2. Traffic Flow Variation during (a) Non-evacuation period and (b) Evacuation period

3.2. Data Exploration

In a typical operating condition, traffic flow shows predictable patterns such as heavy demand during peak hours resulting in high traffic flows. Fig. 2(a) shows the distribution of traffic flow from August 5th, 2017 to August 12th, 2017 for the northbound traffic of I-75. We observe distinct morning peak between 8 am, and 10 am. However, during an emergency event such as a hurricane evacuation, overall traffic condition has to bear severe disruption due to a drastic increase in traffic demand. Drastic oscillation and sudden flow breakdown are the common characteristics of evacuation traffic. Fig. 2(b) shows the distribution of evacuation traffic from September 5th, 2017 to September 9th, 2017. It shows traffic flow variation during the evacuation period of hurricane Irma. We observe that during the evacuation period, overall traffic flow is higher than a regular period with irregular variations and no distinctive morning or evening peak.

As we observe in Fig. 2 (b) we could not extract any traffic data after September 9, 2017, so we are unable to show the traffic flow variation after that time period. Hurricane Irma made its landfall at the Florida Keys on September 10, 2017 as a category 4 storm. Then it passed over several regions of Florida from September 10, 2017 to September 12, 2017. It caused significant power outages, in its path, at several regions in Florida. It took about a week to restore the overall system. So, it is likely that the detectors were malfunctioning, or the data collection server could not retrieve any information during that period.

The roadway segment considered in this study is a three-lane freeway. According to highway capacity manual (National Research Council (U.S.). Transportation Research Board, 2010) the maximum capacity of a freeway segment, under regular condition, should vary from 2000 to 2400 pc/h/ln (passenger car per hour per lane), however these values are applicable only for stable uninterrupted flow condition. From Fig. 2(b), we find that during hurricane Irma traffic condition starts to deteriorate just after the declaration of evacuation order on September 6th, 2017. From September 6th to September 9th, 2017 overall traffic flow is higher than regular traffic condition. Especially from September 7th to September 8th the traffic flow is heavier than rest of the evacuation period; the maximum flows for different roadway segments (i.e. detectors) vary from 4200-5000 vph (vehicle per hour) for all the three lanes combined. Although maximum flow is less than theoretical capacity (3*2000=6000) of the roadway, we observe a significant reduction in overall traffic speed. During Hurricane Irma's evacuation, average traffic speed varies from 40 mph to 60 mph, indicating an unstable traffic flow condition.

To further analyze the prevailing traffic condition, we plot speed vs flow relationship from September 4 to September 9, 2017 which includes both evacuation and non-evacuation periods (see Appendix. B Fig. 8 (a)). In this figure, the red dashed line indicates fundamental speed-flow relationship as a visual guidance (we have not fitted this line to actual data) and the dark dashed line separates between the stable and unstable flow conditions. The upper portion of the horizontal line (see Appendix. B Fig. 8 (a)) indicates stable flow condition, while the lower portion indicates unstable flow condition. In unstable flow condition traffic speed is lower than the free flow speed indicating oversaturated traffic flow. In such condition, the effective roadway capacity will be lower than the theoretical capacity due to interruption in traffic flow (congested condition).

We also plot speed vs. flow relationship (see Appendix. B Fig. 8 (b)) only for the evacuation period from September 7 to September 8, 2017 (when heavy evacuation traffic has been observed). From the figure we find that, during evacuation, the overall traffic is operating either near or below capacity and the observed maximum flow is lower than the theoretical capacity value. A study on Hurricane Ivan (2004), Hurricane Katrina (2005) and Hurricane Gustav (2008) showed that during hurricane evacuation, highway capacity reduces by 35-50% (Dixit and Wolshon, 2014). Hence, comparing the maximum flow values during evacuation with the theoretical capacity under regular condition will be inappropriate due to the difference in the prevailing traffic conditions. To make such a comparison, we need to consider the effective capacity based on prevailing traffic flow condition. It will be interesting to determine, in future studies, to what extent and why the effective capacity is dropping during evacuation.

We also analyze the temporal distribution of total number crashes for I75; Fig. 3 shows the distribution of crashes on different dates during evacuation. We observe that there is an increase in the number of crashes on 6th, 7th, and 8th September which are basically the evacuation period after the declaration of the state of emergency due to Irma. Majority of the crashes during this period were rear-end collisions (about 51%).

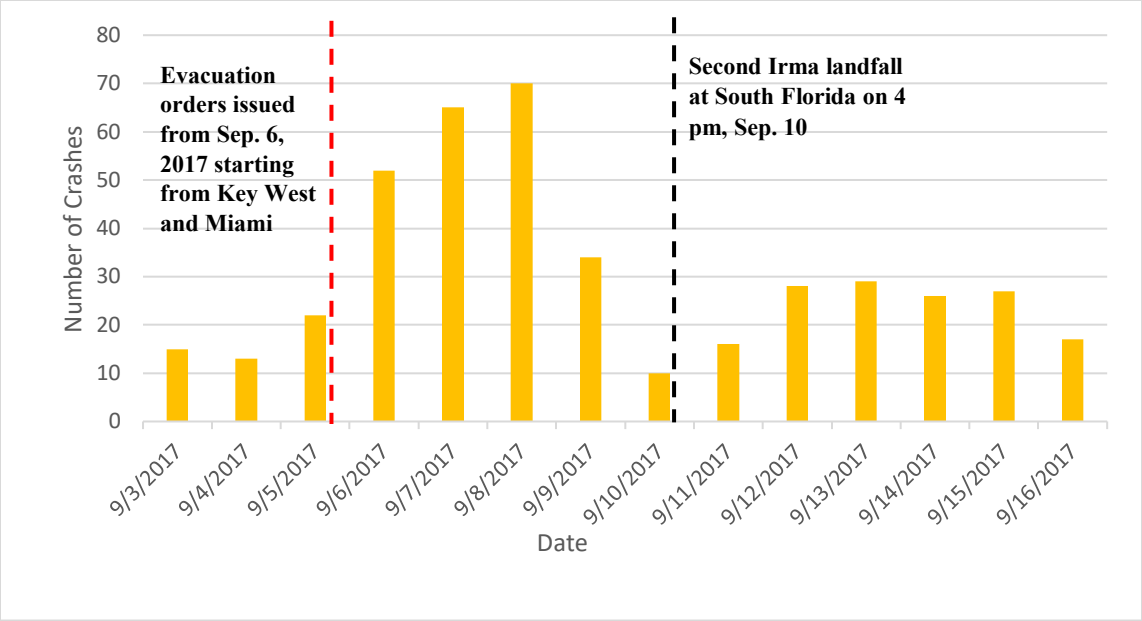

Fig. 3. Number of Crashes during Hurricane Irma Evacuation

3.3. Car-Following Model in SUMO

A car following behavior represents the reaction of the following vehicle with respect to the actions from the leading vehicle, where both vehicles are driving in the same lane. To replicate car following behavior in a simulation environment, researchers have been using different car-following models such as IDM, Wiedemann Krauss, etc. These models represent the driver's behavior (e.g., brake, accelerate) based on the interaction between leading and following vehicles.

In this study, we develop a micro-simulation model of evacuation traffic in SUMO (29) version 1.2.0. We use a collision-free model Krauss (Kraus, 1998), which is the default car-following model for SUMO. Though the Intelligent Driver Model (IDM) has been widely used for car-following modeling, studies have shown that the IDM provides greater errors in speed than Krauss model for unsteady traffic conditions, especially for car and heavy vehicles (Kanagaraj et al., 2013). Because IDM does not perceptibly follow the speed changes of the preceding vehicle (Milanés and Shladover, 2014) in an unsteady state. The Krauss model is a microscopic, space continuous car-following model, which is a stochastic version of the Gipps model (M. Treiber and Kesting, 2013). The model was developed by Krauss in 1997 based on the concept of safe speed, where the safe speed is computed as follows:

$$v_{safe} = v_n(t) + \frac{g(t) - v_n(t)\tau}{\frac{v_n(t) + v_{n-1}(t)}{2b_m} + \tau} \quad (1)$$

where, $v_{n-1}(t)$ *and* $v_n(t)$ represent the speeds of the leading and following vehicles at time t, $g(t)$ is the gap to the leading vehicle at time t, τ is the driver's reaction time (about 1s) and b_m is

the maximum deceleration of the vehicle (m/s^2). In a car following scenario, v_{safe} can be larger than the maximum speed (v_{max}) allowed on the road or larger than the vehicle's physical acceleration capabilities. To prevent this scenario, the desired speed of the vehicles is calculated. The desired speed (v_d) of each vehicle is the minimum of the safe speed v_{safe}, the current speed plus the maximum acceleration and the maximum speed (Bieker-Walz et al., 2017):

$$v_d(\mathrm{t}) = min\left[v_{safe}(t), v_n(t) + a\tau, v_{max}\right] \quad (2)$$

To account the human error-related imperfection for human drivers, a random error (σ_a) was subtracted from the desired speed

$$v_n(t) = max\left[0, rand[v_d(t) - \sigma_a, v_d(\mathrm{t})]\right] \quad (3)$$

We use the Krauss model to simulate human-driven vehicles in SUMO. The default parameters for the model can be found in ("Simulation of Urban Mobility: Vehicle Type Parameter Defaults," 2019). To select the base model, we reviewed several studies, though all the studies were done for regular traffic conditions. We use these parameter values in our initial model (see Table 1). Through the calibration process, we change these parameters to represent the evacuation condition. Here the parameter sigma has been introduced to model driver's imperfection to adapt to the speed of a traffic stream. If the value of sigma (σ_a) is above 0, drivers with the default car-following model will drive slower than possible safe speed, and the value will be chosen from a random distribution between [0, acceleration]. Whereas tau (τ) indicates the reaction time for the drivers which varies from 1.0 to 1.5 sec.

In a traffic stream, the desired driving speed usually varies for different vehicles. This can be modeled by defining the attribute "speed factor," which allows a vehicle to draw "speed factor" from a normal distribution. This parameter can be given as "norm (mean, dev)" or "normc (mean, dev, min, max)." For instance, if we choose the speed factor as "normc (1, 0.1, 0.2, 2)", then it will result in a speed distribution where 95% of the vehicles drive between 80% and 120% of the legal speed limit.

Table 1
Initial Model before Adjusting the Parameters

Vehicle Types	Max Speed (m/s)	Speed Factor norm (mean, deviation, min, max)	Min Gap (m)	Car Following Model	Max Accel (m/s^2)	Max Decel (m/s^2)	Sigma	Tau (s)
PC	70	normc(1,0.1,0.2,2.0)	3.0	Krauss	3.0	5.5	0.5	1.0
HGV	65	normc(1,0.1,0.2,2.0)	3.0		3.0	5.5	0.5	1.0

3.4 ACC Controller

We select the ACC driving model based on (Liu et al., 2018; Milanes et al., 2014; Milanés and Shladover, 2016, 2014; Xiao et al., 2017), where the ACC control algorithm is divided into three modes based on three different motion purposes: (i) the cruising (or speed) control mode is designed to maintain the drivers' chosen desired speed, (ii) the gap control mode aims to maintain a constant time gap between the controlled vehicle and its predecessor, and (iii) the gap-closing controller enables the smooth transition from speed control mode to gap control mode. Later, TransAID (Mintsis, 2018) has introduced a fourth mode (i.e. collision avoidance mode) to the controller that prevents rear-end collisions when safety critical conditions prevail. The selected parameters for the ACC car following model is shown in Table 2. We present the basic definitions and equations for these four ACC control modes in Appendix A.

Table 2
Controller Parameters for ACC

Parameters	Value	Remarks
Speed Control Gain	0.4 s^{-1}	Cruising Model
Gap Control Gain Space	0.23 s^{-2}	Car following Model
Gap Control Gain Speed	0.07 s^{-1}	Car following Model
Gap Closing Control Gain Space	0.04 s^{-2}	Approaching Model
Gap Closing Control Gain Speed	0.80 s^{-1}	Approaching Model
Collision Avoidance Gain Space	0.8 s^{-2}	Collision Avoidance Model
Collision Avoidance Gain Speed	0.23 s^{-1}	Collision Avoidance Model

3.5. SUMO Simulation Model Development and Calibration

To design simulation experiments in SUMO, we would need a well-calibrated model. This requires representing the real-world network in the simulation environment with proper geometric features. To replicate the real-world scenario, we imported the traffic network for I-75 from the Open Street Map and converted this network into the sumo network file. We simulate a 9.5-mile-long segment between Ocala to Gainesville, which includes two entry and exit ramps. We have adjusted the traffic network using the SUMO network editor and removed all the unnecessary routes and nodes.

In the simulation, we include two types of vehicles: passenger car (PC) and heavy goods vehicle (HVG). We do not have the exact distribution of PC and HGV for that study period. However, most of the cases the HGV percentages vary from 2 to 5% of the total number of vehicles. For our simulation, we assume the HGVs as 4%, which would be adjusted during the calibration process. We get the traffic volume from the RITIS database at 20 to 30-second resolution and aggregate them into 5 min interval and convert this volume into 5 min average flow. Since we are simulating a 2-hour period, we input the average interval flow for 2 hours. From the analysis, we find that the

maximum number of crashes occurred on September 8, 2017, between 2 pm and 5 pm. Therefore, we have chosen the time window of 1:30 to 3:30 pm for our simulation experiments. After excluding the first 30 minutes of simulation warm-up time and last 30 minutes of cool-down time (no statistics were collected during this time), simulation data of 60 minutes (2-3 pm) were used for calibration and validation.

For calibrating the model, we add 8 loop detectors on the network exactly at the same location as the MVDS detectors (see Fig. 1). The default output frequency from SUMO is 1sec; however, we can adjust this value by changing the default settings. In our case, we obtain aggregated volume and average speed for 5-min intervals from the loop detectors. We use Geoffrey E. Heaver (GEH) statistics (Bash, 2012), modified chi-square statistics to compare the filed volume with the simulation. GEH statistics incorporate both relative and absolute differences between the two groups. The GEH can be stated as follows:

$$GEH = \sqrt{\frac{2 * \left(M_{obs}(n) - M_{sim}(n)\right)^2}{(M_{obs}(n) + M_{sim}(n))}} \quad (4)$$

We calculate the GEH for each detector (i.e., 8 detectors) and each time interval (i.e., 2:00 pm to 3:00 pm, in total 12 intervals). We also calculate the Root Mean Square Error (RMSE) and Root Mean Square Percentage Error (RMSPE). To check the compatibility of the developed model, we reviewed several specifications. However, all of the specifications for calibrating a traffic simulation model is given for regular traffic condition. For an evacuation period, traffic variation is significantly higher than a regular period, and it is difficult to achieve better accuracy. So, there should be a different set of guidelines for calibrating models for the evacuation period. We still follow the standards mentioned in (Nezamuddin et al., 2011), which recommend for 85% of the data point the GEH value should be less than 5, and the absolute speed difference (ASD) between simulated speeds and field speeds should be within 5 mph (or 2.5 m/s). So, our objective is to keep the GEH less than 5 and absolute speed difference below 2.5 m/s.

First, we select the speed distribution of vehicles based on the field measurement, which is slightly adjusted during the calibration process. We change each parameter within a specific range, which has been selected based on previous studies and engineering judgment (Table 3).

Table 3

Parameter ranges for model calibration process

Types	Proportion (%)	Min Gap (m)	Max Accel. (m/s^2)	Max Decel. (m/s^2)	Sigma	Tau (s)
Car	[96,97,98]	[2.0, 2.5 3.0]	[3.0, 3.5,	[5.0,5.5,6.0,6.5 7.0,7.5]	[0.1,0.2,0.3,0.4,0.5]	[1.0,1.2,1.3,1.4 1.5]

			4.0, 4.5]			
HGV	[2, 3, 4]	[2.0, 2.5 3.0]	[3.0. 3.5, 4.0 4.5]	[5.0,5.5,6.0,6.5]	[0.1,0.2,0.3,0.4,0.5]	[1.0,1.2,1.3,1.4 1.5]

When calibrating the model we perturb each parameter and run the simulation 10 times with random seeds to observe the variations in GEH, ASD, RMSE and RMSPE values. In total we run the simulation 260 times ($3 * 10\,[vehicle\ proportion] + 3 * 10\,[Min\ Gap] + 4 * 10\,[Max\ Accel.] + 6 * 10\,[Max\ Dccel.] + 5 * 10\,[Sigma] + 5 * 10\,[Tau]$) based on the ranges of different parameters. Due to the large variation of speed and flow, it is challenging to achieve better accuracy levels for simulating evacuation traffic. We present the final parameters for the model in Table 4. We run the final model 10 times with random seeds and each time we estimate the GEH, ASD, RMSE, and RMSPE. Finally, we estimate the average value for each of these metrics (Table 5). About 73% of the observations show a GEH value of less than 5 and ASD value below 2.5 m/s. Moreover, RMSE for speed is less than 5m/s, which indicates the model is reasonably calibrated to capture the speed variations occurring during an evacuation period. As shown in Fig. 2, there is some drastic change in traffic speed at certain points, which induce a large error in our model (high absolute difference). We are unable to capture this variation with the simulation model. Evacuation traffic modeling is a challenging task that requires different standards and specifications to check the performance of the calibrated model. However, currently, such standards do not exist for evacuation traffic simulation models.

In our final model (see Table 4), values of maximum acceleration and deceleration are higher than the regular car-following model for normal traffic conditions. This indicates that abrupt changes in speeds and a higher rate of acceleration are typically followed in the evacuation. In a stop and go traffic condition, drivers are more likely to take every opportunity to accelerate to recover the delays induced by a repetitive breakdown in traffic flow. In case of minimum gap (Min Gap) parameter, previous studies have used different values ranging between 2 and 4m to simulate traffic for regular condition (Li et al., 2017b; Martin Treiber and Kesting, 2013). However, there is no specific guideline to choose the minimum gap parameter for the car following model for evacuation traffic conditions. Selection of the minimum gap value is critical. If the minimum gap is very low, it will produce an unrealistically high value of deceleration. Considering this issue, we use minimum gap value between 2.0 and 3.0m when calibrating the model. Moreover, several studies (Li et al., 2017a) have used minimum gap of 2.0m while modeling congested stop and go traffic condition to represent realistic driving behavior. From the model calibration result, we find the minimum gap parameter value as 2.0 m. This is plausible since in a highly congested condition such as evacuation, drivers are more likely to reduce the gap from the leading vehicle. Also, drivers attempt to maintain a minimum time gap of tau between the rear bumper of their leader and their front-bumper. In our case, the value of tau is 1.2, which is less than the usual reaction

time of 1.5 sec under a regular traffic condition. These changes in parameters from a regular traffic condition, however, indicate potential crash risks during evacuation.

Table 4
The Final Model after Adjusting the Parameters

Types	Proportion	Max Speed (m/s)	Speed Factor norm (mean, deviation, min, max)	Min Gap (m)	Car Following Model	Max Accel. (m/s^2)	Max Decel. (m/s^2)	Sigma	Tau (s)
PC	98 %	70	normc(0.96,0.3,0.2,1)	2.0	Krauss	4.5	6.5	0.2	1.2
HGV	2%	65	normc(0.96,0.3,0.2,1)	2.0		4.5	6.5	0.2	1.2

Table 5

Values of the performance metrics for the calibrated model

Metrics	Average Values for Flow	Metrics	Average Values for Speed
GEH <5	72.9 % of the total observations	ASD <2.5 m/s	73.2% of the total observations
RMSE	278.863	RMSE	4.738
RMSPE	12.312	RMSPE	20.76

3.6. Surrogate Safety Measures

A simulated environment does not explicitly show the collisions between two interacting vehicles. Hence, we need some surrogate measures to represent interactions between vehicles in a traffic stream and to identify potentially unsafe conditions. To evaluate crash risks from simulation models, previous studies have used several surrogate safety measures such as time to collision (TTC), post encroachment time (PET), rear-end crash risk index, deceleration rate to avoid a collision (DRAC). In this study, we are using one temporal proximity-based indicator (TTC) and one deceleration-based indicator (DRAC) to evaluate the impact of ACC equipped vehicles on crash risks. However, in absence of these measures we can also use the variance of speed. A higher variance in speed would indicate an unstable traffic stream, and consequently a potential collision scenario. To implement this approach at a micro level, we have to track speed variations (e.g., speed variance) of each vehicle and check if there is a sudden reduction in speed. This process would take more time and resources in processing the outcome to estimate the number of potential collisions. In our study, we followed a similar approach. Instead of directly using the speed variance, we use a sophisticated measure DRAC to automatically indicate an abrupt decrease in traffic speed in case of a potential collision. Since, DRAC is derived from speed variations, we believe that both approaches will produce a similar outcome.

The TTC measure, first introduced by Hayward (Hayward, 1972), is defined as the expected time for two vehicles to reach a common position on the road, given that their speed and trajectory remain the same. If the following vehicle *n* moves faster than the preceding vehicle (*n-1*), then TTC can be evaluated by using Equation 5.

$$TTC_n(t) = \begin{cases} \frac{x_{n-1}(t) - x_n(t) - L_{n-1}}{v_n(t) - v_{n-1}(t)}, if\ v_n(t) > v_{n-1}(t) \\ \infty, if\ v_n(t) < v_{n-1}(t) \end{cases} \quad (5)$$

where $TTC_n(t)$ denotes the TTC value of the vehicle n at time t and x, v, L denote the position, speed, and length of the corresponding leading $(n-1)$ and following (n) vehicles, respectively. Researchers have used different threshold values (1.0, 1.5, 2.0, etc.) of TTC to identify whether two vehicles will collide or not (Essa and Sayed, 2015; Guo et al., 2019; Li et al., 2017c, 2017b, 2017a; Liu et al., 2018; Wang and Rajamani, 2004). Van der Horst (Van Der Horst and Hogema, 1993) suggested that the preceding vehicle and following vehicle are assumed to be in a collision if the TTC value for the following vehicle is less than 1.5.

In an oscillatory traffic condition (stop and go traffic) deceleration-based indicator are more critical. So, we are using the deceleration rate to avoid a collision (DRAC) to consider the effect of speed differentials and decelerations on crash risks. DRAC, first introduced by Cooper and Ferguson (Cooper and Ferguson, 1976), indicates the maximum deceleration rate needed to be applied by a vehicle to avoid the collision with another conflicting vehicle. In the case of a car following scenario, the preceding vehicle $(n-1)$ is responsible for initiating action such as braking, lane changing, etc. while the following vehicle (n) has to react to this action by braking. For this rear-end interaction, the DRAC for the following vehicle n can be expressed as follows:

$$DRAC_n^{REAR} = \frac{\left(v_n(t) - v_{n-1}(t)\right)^2}{2[(x_{n-1}(t) - x_n(t)]} \quad (6)$$

Where v, x denote the speed and position of the corresponding leading $(n-1)$ and following (n) vehicles, respectively. Several studies have recognized the relevance of DRAC to measure crash risk and crash severity. They have also introduced different severity levels based on a different range of DRAC values. The American Association of State Highway and Transportation Officials (AASHTO) (*A Policy on Geometric Design of Highways and Streets*, 2011) recommends that the maximum comfortable deceleration rate for most of the drivers is $3.4\ m/s^2$. Archer (Jeffery Archer, 2005) suggested that if, for a given vehicle interacting with a preceding vehicle, the maximum DRAC value is greater than $3.35\ m/s^2$, the vehicle is assumed to be in a collision with the preceding vehicle. In this study, we use the threshold values for TTC as 1.5 sec and for maximum DRAC as $3.30\ m/s^2$.

4. Results

To estimate the surrogate safety assessment measures, we equip the vehicles with SSM (surrogate safety measures) ("Simulation of Urban Mobility: Simulation/Output/SSM Device," 2019) devices. Each SSM device provides an estimate of time to collision (TTC) and maximum deceleration rate to avoid a collision (maximum DRAC) value for the study corridor. To identify the number of conflicts that can lead to potential traffic collisions, based on previous studies, we choose threshold values for TTC and maximum DRAC as 1.5 sec and 3.30 m/s^2, respectively. This means that if TTC and maximum DRAC value between the leading and preceding vehicle is less than the threshold value of TTC and greater than the threshold value of maximum DRAC we identified it as a potential collision.

Fig. 4 and 5 illustrate the distributions of maximum DRAC and TTC values for the base condition and 25% MPR of ACC vehicles for a single simulation run. Fig. 4 shows that maximum DRAC values for the evacuation traffic mostly vary from 3.2 to 4.5 $\mathrm{m/sec^2}$ and TTC values vary from 0.5 to 1.5 sec. It is reasonable to choose 3.30 $\mathrm{m/sec^2}$ as the threshold value of maximum DRAC and 1.5 sec as the threshold value of TTC to assess the impact of ACC vehicles. Considering these thresholds, we observe a significant number of potential collisions (TCC value less than 1.5 sec, while the maximum DRAC value greater than 3.30 m/sec^2) for the base condition (i.e., without ACC vehicles). However, after we introduce the ACC vehicles (25% MPR), most of the cases the TCC values increase while the maximum DRAC values decrease, indicating improvement in overall safety condition.

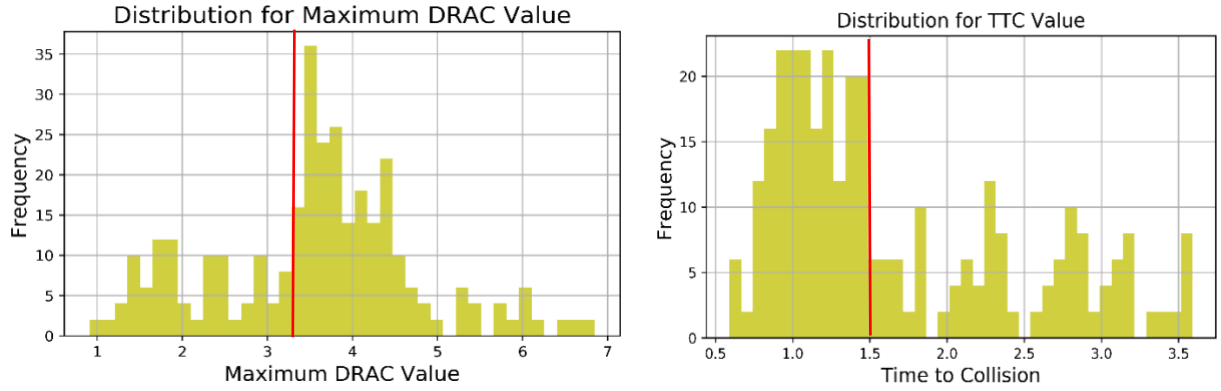

(a) (b)

Fig. 4. Distribution of (a) maximum DRAC values (greater 1 m/sec^2) (b) TTC values (less than 4 sec) for base condition; red line indicates the critical values for DRAC = 3.30 $m/sec^2$and TTC = 1.5 sec

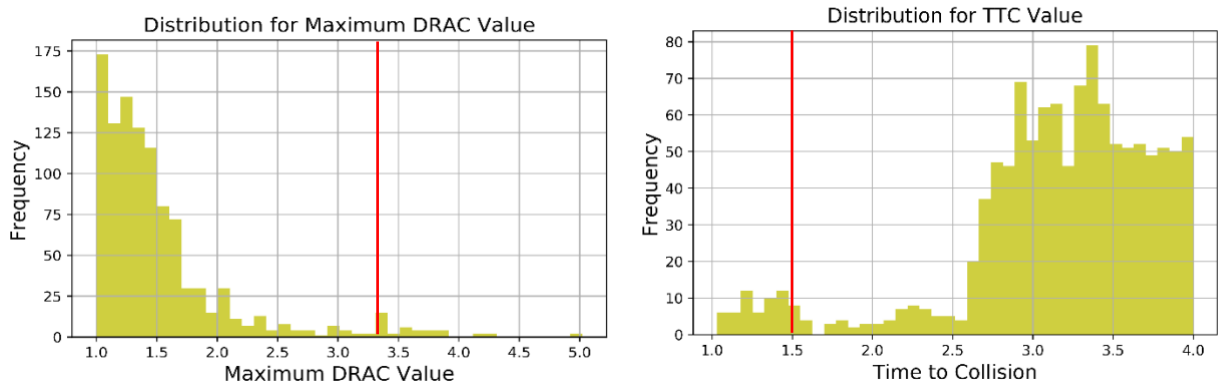

(a) (b)

Fig. 5. Distribution of (a)maximum DRAC values (greater 1 m/sec^2) (b) TTC values (less than 4 sec) at 25% MPR of ACC vehicles (time headway =1.3 sec); red line indicates the critical values for maximum DRAC = 3.30 $m/sec^2$and TTC = 1.5 sec

To estimate the variation in result, we run the final simulation 10 times with random seeds to eliminate any random effect. For each simulation run, we estimate the number of potential collisions and report the average value aggregating all the results for different simulation runs. From simulation results, we find that the average number of conflicts leading to potential collisions for the base condition is 264. We follow the same procedure to estimate the number of potential collisions for different levels of market penetration of ACC-equipped vehicles.

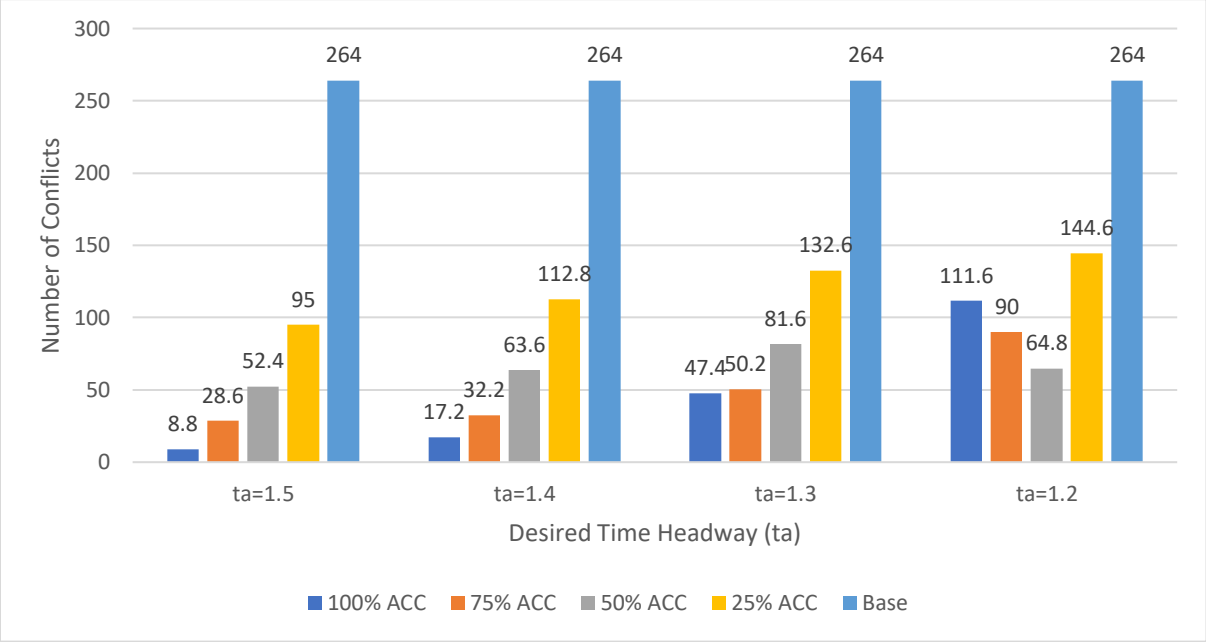

Fig. 6. Variation of Number of potential collisions for different values of desired time headway

In an ACC system, the controlling parameters allow a vehicle to maintain a constant gap with the preceding vehicle. Hence, by fixing the desired headway, the ACC-equipped vehicle can maintain

a safe cruising distance. Moreover, the reaction time for the ACC equipped vehicle (0.1 sec) is less than a manually driven vehicle, consequently desired time headway (1.1 to 1.6 sec) is also less than manual vehicle (1.5 sec) (Porfyri et al., 2018). In this experiment, we choose 4 levels of market penetration of ACC-equipped vehicles and use 4 values of desired time headway. At a given market penetration, we run the simulation with four different values of desired time headway, and for each case, we estimate the TTC and maximum DRAC values. The experiment result shows that if we fix the desired time headway greater than 1.2 sec, the number of potential collisions decrease with the increase in the penetration rate of ACC equipped vehicle (see Fig. 6). When the desired time headway is 1.2 sec, the result shows some discrepancies. For instance, the number of conflicts leading to potential collisions decreases with the increase in MPR of ACC equipped vehicles up to 50%, but after that it increases with the increase of ACC equipped vehicles. However, the number of potential collisions always remains less than the base condition.

To measure the difference between the base conditions with the other scenarios we perform a two-sample *t*-test and report the significance of these differences (*p*-value). In Table 6, we present the *t*-test results for ACC equipped vehicles with the desired headway of 1.3 sec. From the result, we observe that with only 25% market penetration rate of ACC vehicle we can achieve about 49.7% reduction in the number of potential collisions. Further improvement can be achieved at 75% market penetration rates of ACC equipped vehicles. Reduction in the number of potential collisions is almost the same (around 80%) for both 75% and 100% MPR. We have also conducted the same analysis with different values of the desired headway, and for each case, we have seen similar outcomes.

Table 6

Percentage change in the number of potential collisions averaged over 10 simulation runs (desired time headway is 1.3 sec)

	Estimate	Value	Mean Difference	% Change in mean value	*p*-value	Lower bound	Upper bound
Base (no ACC)	mean	264	---	---	---	---	---
	standard deviation	51.29					
Base + 25% ACC	mean	132.6	131.4	49.7%	<0.0001	119.53	208.06
	standard deviation	23.02					
Base + 50% ACC	mean	81.6	182.4	69%	<0.0001	145.00	227.79
	standard deviation	12.39					
Base + 75% ACC	mean	50.2	213.80	81%	<0.0001	179.12	248.47
	std standard deviation	9.64					

100% ACC	mean	47.4	216.60	82%	<0.0001	181.43	251.76
	standard deviation	13.06					

Moreover, we performed a sensitivity analysis to understand the impact of gap control parameters of the ACC vehicles over the changes in potential collision. We experimented with different combinations of gap control gain space (k_2) and gap control gain speed (k_3) values. Table 7 presents the percentage change in the number of potential collisions for different combinations of gap control parameters. We observe that increasing the value of k_2 from 0.1 to 0.5 decreases the number of potential collisions. However, in case of k_3, the changes are rather irregular. Overall, for each combination of gap control parameters, the number of potential collisions is significantly lower than the base condition. Although we experimented with different combination of gap control parameter, selecting the optimal gap control parameters is challenging which requires individual vehicle level data such as acceleration, deceleration, gap acceptance etc. However, we do not have such information, hence we use the existing parameters which are practically possible based on field experiments to run the model (Table 2).

Table 7

Sensitivity analysis to demonstrate the changes in the number of potential collisions for different combinations of gap control parameters (Gap Control Gain Space [k_2] and Gap Control Gain Speed [k_3]); the number of potential collisions is averaged over 10 simulation runs, each simulation includes 25% MPR of ACC vehicles with desired time headway of 1.3 sec.

		Estimates	Gap Control Grain Speed (k_3)				
			0.05	0.06	0.07	0.08	0.09
Gap Control Gain Space (k_2)	0.1	Number of potential collisions	114.0	137.7	125.8	114.0	134.6
		Standard deviation	17.9	30.51	17.8	10.3	17.3
		Percentage change compared to base condition	56.8 %	47.8 %	52.4 %	56.8%	49.1%
	0.2	Number of potential collisions	114.0	131.1	133.8	131.0	114.0
		Standard deviation	14.4	19.5	25.2	23.2	12.4
		Percentage change compared to base condition	56.8 %	50.3%	49.3%	50.4%	56.8%
	0.3	Number of potential collisions	112.4	123.7	113.8	128.6	121.4
		Standard deviation	16.7	25.8	15.4	18.4	16.0
		Percentage change compared to base condition	57.4%	53.2%	56.9%	51.3%	54.0%
	0.4	Number of potential collisions	111.4	113.5	109.9	116.4	112.8

	Standard deviation	10.9	16.8	20.5	22.1	20.6
	Percentage change compared to base condition	57.8%	57.0%	58.4%	59.9%	57.3%
0.5	Number of potential collisions	105.4	109.8	101.0	109.4	109.3
	Standard deviation	16.7	26.9	16.6	23.2	17.9
	Percentage change compared to base condition	60.2%	58.4%	61.7%	58.6%	58.6%

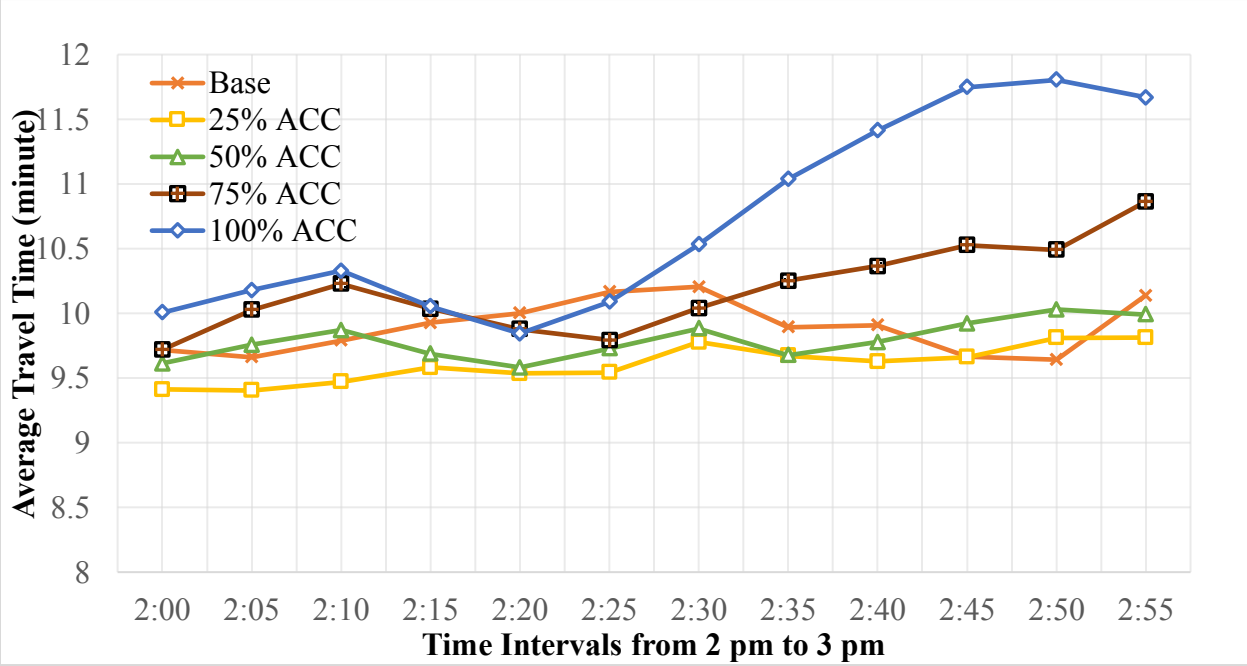

Fig. 7. Travel Time Variation at Different Market Penetration Rate of ACC vehicles

We have also collected the average travel time for the base scenario as well as for different MPR of ACC equipped vehicles. We have observed that, with the increase in the percentage of ACC equipped vehicles, average travel time reduces from the base condition. However, for 75% or 100% MPR of ACC, the travel time increases (Fig.7) The average travel time for the base condition is 9.7 minute, whereas at 100% MPR of ACC equipped vehicles average travel time is 10.8 minutes. This variation can be attributed to the fact that the ACC system decreases the sudden changes in the rate of acceleration, which reduces the sharp changes in traffic speed. Consequently, the overall speed reduces to adapt to the traffic stream.

5. **Discussion**

This study has certain limitations. Our findings rely on simulation experiments that do not fully mimic real-world evacuation traffic conditions. In this study, we only calibrated the simulation

model with real evacuation traffic data, which shows a disperse distribution for speed. It is challenging to select an accurate distribution of speed to match the speed variation of the simulated vehicles with real-world data. To check the performance of our model, we have used GEH statistics and absolute speed difference. We find that for 72.9% of the observations the GEH score is less than 5, whereas existing standards recommend for 85% of the data points the GEH value should be less than 5 in normal operating condition. During evacuation we observe an abrupt change in traffic flow due to the large volume of evacuation traffic from surrounding areas, hence in some portion of the roadway segment (mostly entry ramps) we observe significantly higher traffic volume compared to average traffic volume of the entire roadway segment. However, in the simulation environment the roadway capacity remained similar for all the segments, hence, in some portion of the roadways the simulated traffic volume fails to match with actual traffic volume. That is why the GEH test fails to achieve the recommended result. One of the possible ways to overcome this issue could be breaking down the model into smaller roadway segment to see if it generates more reliable results in terms of calibration. Moreover, recommended standards for these metrics are very conservative and are generally suitable only for normal traffic conditions. We, therefore, believe that new guidelines should be developed to calibrate traffic simulation models for evacuation traffic scenarios.

Although existing microsimulation models are more advanced, they rely on collision free models. Thereby, they fail to simulate collisions and generate features to assess the safety of different simulated traffic scenarios (Essa and Sayed, 2020). As a solution to this problem, following existing literature, we have utilized surrogate safety measures (SSM) such as time to collision (TTC) and deceleration rate to avoid a collision (DRAC) to assess the safety impacts of evacuation traffic. However, these methods have some limitations. First, obtaining reliable conflict results requires a rigorous calibration of the simulation model. Second, simulation models may fail to accurately represent actual driving behavior during evacuation, hence they may fail to generate near misses. A two-stage calibration process involving a rigorous calibration of the simulation model and safety-oriented calibration ensuring collisions are correctly generated can improve the representativeness of the simulated data (Papadoulis et al., 2019). However, it is challenging to obtain high resolution data related to traffic conflicts (i.e., minimum gap, near miss) from real-world sources, particularly during hurricane evacuation.

The results of this study are intuitive and based on the data collected from a real-world evacuation scenario (Hurricane Irma). We found that during evacuation scenario the roads operate near capacity for a long period of time due to heavy traffic demand. For similar evacuation traffic condition, we anticipate that these results will be representative. However, data from multiple hurricanes are needed to study the transferability of the results. Future studies can analyze evacuation data from multiple hurricanes across different regions to confirm the transferability of these results.

6. Conclusion

Managing evacuation traffic is an enduring transportation challenge due to uncertainty and drastic changes in traffic states (Murray-Tuite and Wolshon, 2013). During evacuation, drivers have to face stop-and-go traffic conditions. These types of irregularities and oscillatory traffic behavior increase the chances of driver's perception related errors. In this study, we calibrated a microscopic traffic simulation model to analyze driving behavior during evacuation. The model has been calibrated using real-world evacuation traffic data collected during Hurricane Irma. For the calibrated model, the values of maximum acceleration and deceleration were found to be 4.5 m/s^2 and 6.5 m/s^2, respectively. These values are quite greater than those in typical car-following models calibrated under regular traffic conditions. Also, larger acceleration and deceleration values indicate abrupt speed variation, which is the most common scenario for evacuation traffic.

Using the calibrated micro-simulation model, we evaluated the safety impacts of ACC equipped vehicles on crash risks. Adopting two surrogate safety measures TTC and maximum DRAC, we have found that ACC-equipped vehicles can significantly reduce the number of potential collisions during evacuation. The experiment results also indicated that the safety impact of the ACC system largely depends on its parameter settings of ACC controllers. By fixing the desired time headway at a value greater than 1.2 sec, the number of potential collisions can be reduced by 49.7%. At the same time, we have also found that if we keep the MPR of ACC vehicles below 50%, then average travel time improves over the base condition. This is a promising result considering that an MPR of 25% to 50% of ACC vehicles is more likely in the future compared to 75% to 100% MPR of ACC vehicles.

Our study has several implications. First, using real-world evacuation traffic data, we have established that typical parameters of car-following models should be adjusted to account for an evacuation condition. Researchers and practitioners should consider our findings when using micro-simulation tools for modeling evacuation traffic. Second, this study evaluates the safety impact of different driving assistance systems on crash occurrence during evacuation. The findings are promising as it was shown that the ACC system could potentially reduce the number of crashes during evacuation. It is worth noting that most modern cars are equipped with an ACC system. However, the lack of public knowledge on how to use them as well as the high level of mistrust in such emerging technology discourage drivers from using this type of vehicle driving assisting system (Kamalanathsharma et al., 2015). Transportation and emergency management agencies should take necessary steps to acquaint drivers with new in-vehicle technologies and their potential benefits in an emergency situation such as hurricane evacuation.

Moreover, this study opens new directions for future research. For instance, future work should assess the safety and mobility impact of connected vehicles with platooning and cooperative adaptive cruise control systems. Studies should also investigate the impact of vehicle to vehicle (V2V) and vehicle to infrastructure (V2I) communication technologies on reducing potential crash risks during an emergency evacuation. Finally, as we have identified the limitations of simulation experiments, field experiments are necessary before deploying our recommendation in a real-world hurricane evacuation scenario.

Acknowledgment

The research presented in this paper is supported by Safety Research using Simulation University Transportation Center (SAFER-SIM) and the U.S. National Science Foundation grant CMMI-1917019. SAFER-SIM is funded by a grant from the U.S. Department of Transportation's University Transportation Centers Program (69A3551747131). However, the U.S. Government assumes no liability for the contents or use thereof.

Appendix A. car-following model for ACC equipped vehicles

Speed Control Mode

The speed control mode is activated when there are no preceding vehicles (n) in the range covered by the sensors, or preceding vehicles exist in a spacing larger of 120 m (Liu et al., 2018; Xiao et al., 2017). This mode aims to eliminate the deviation between the vehicle speed and the desired speed and is given as:

$$\alpha_{n-1}(t+1) = k_1\big(v_d(t) - v_{n-1}(t)\big), k_1 > 0 \quad (7)$$

Where $\alpha_{n-1}(t+1)$, represents the acceleration for the following vehicle for the next time step $(t+1)$ recommended by the speed control mode; $v_d(t)$ and $v_{n-1}(t)$ denotes the desired cruising speed and the speed of the follower $(n-1)$ at the current time step (t); k_1 is the control gain parameter determining the rate of speed deviation for acceleration, which varies in between $0.3 - 0.4s^{-1}$ (Xiao et al., 2017); in this study we choose $0.4s^{-1}$.

Gap Control Mode

When the gap control mode is activated, the acceleration in the next time step $t+1$ is represented as a second-order transfer function based on the gap and speed deviations with respect to the preceding vehicle, which can be defined as follows,

$$\alpha_{n-1}(t+1) = k_2 e_{n-1}(t) + k_3(v_n - v_{n-1}), k_2, k_3 > 0 \quad (8)$$

Here, $e_{n-1}(t)$ is the gap deviation of the following vehicle at the current time step t, and, $v_n(t)$ and $v_{n-1}(t)$ are the current speed of the preceding and following vehicles; k_2 and k_3 are the control gains on both the positioning and speed deviations, respectively. Xiao et al (Xiao et al., 2017) proposed values for the control gains, $k_2 = 0.23s^{-2}$ and $k_3 = 0.07s^{-1}$. The gap control mode is activated when the gap and speed deviations are concurrently smaller than 0.2 m and 0.1m/s respectively (Xiao et al., 2017). The gap deviation of follower vehicle $\big(e_{n-1}(t)\big)$ is defined as,

$$e_{n-1}(t) = x_n(t) - x_{n-1}(t) - \tau_d v_{n-1}(t) \quad (9)$$

According to Equation (9), the gap deviation is calculated by the current position of the preceding vehicle $x_n(t)$, the current position of the following vehicle is $x_{n-1}(t)$ and the desired time gap τ_d of the ACC controller.

Gap-closing Control Mode

The initial ACC car-following models developed by (Milanés and Shladover, 2016) do not consider the ACC longitudinal vehicle response under gap closing mode. Later, Xiao et al. (Xiao et al., 2017) overcome this shortcoming introducing a gap-closing controller by tuning the parameters of the existing gap controller. In this study we also adopt the gap-closing control mode, which is triggered when the spacing to the preceding vehicle is smaller than 100m. For gap closing control, the control gains of Equation (8) are set as $k_2 = 0.04s^{-2}$ and $k_3 = 0.8\,s^{-1}$ (Mintsis, 2018). If the spacing between leading and following vehicle is between 100m and 120m, the controlled vehicle retains the previous control strategy (Gap Control mode) to initiate hysteresis in the control loop performing smooth transfer between the two strategies (Gap control and gap closing control) (Liu et al., 2018; Xiao et al., 2017).

Collision Avoidance Mode

TransAID (Mintsis, 2018) introduced the collision avoidance mode into the ACC car-following model to prevent rear-end collisions occurring during simulations. These control model activated when safety critical conditions arise which means low time-to-collision (TTC) values, or a follower's speed significantly higher than its leader's. Collision avoidance controller is derived by tuning the parameters of the existing gap controller and it get activated when the spacing to the preceding vehicle is lower than 100m, the gap deviation is negative, and the speed deviation is smaller than 0.1m/s. Based on (Mintsis, 2018) we set the gain values as $k_2 = 0.8s^{-2}$ and $k_3 = 0.23s^{-1}$ to ensure that ACC vehicles break hard enough to avoid an imminent collision. Similar to previous case the controlled vehicle retains the gap control strategy when the spacing between leading and following vehicle is between 100m to 120m, to provide hysteresis in the control loop and perform a smooth transfer between the two strategies (Gap control and collision avoidance control) (Liu et al., 2018; Xiao et al., 2017).

Appendix B. Traffic Speed vs. Flow relationship for different traffic conditions

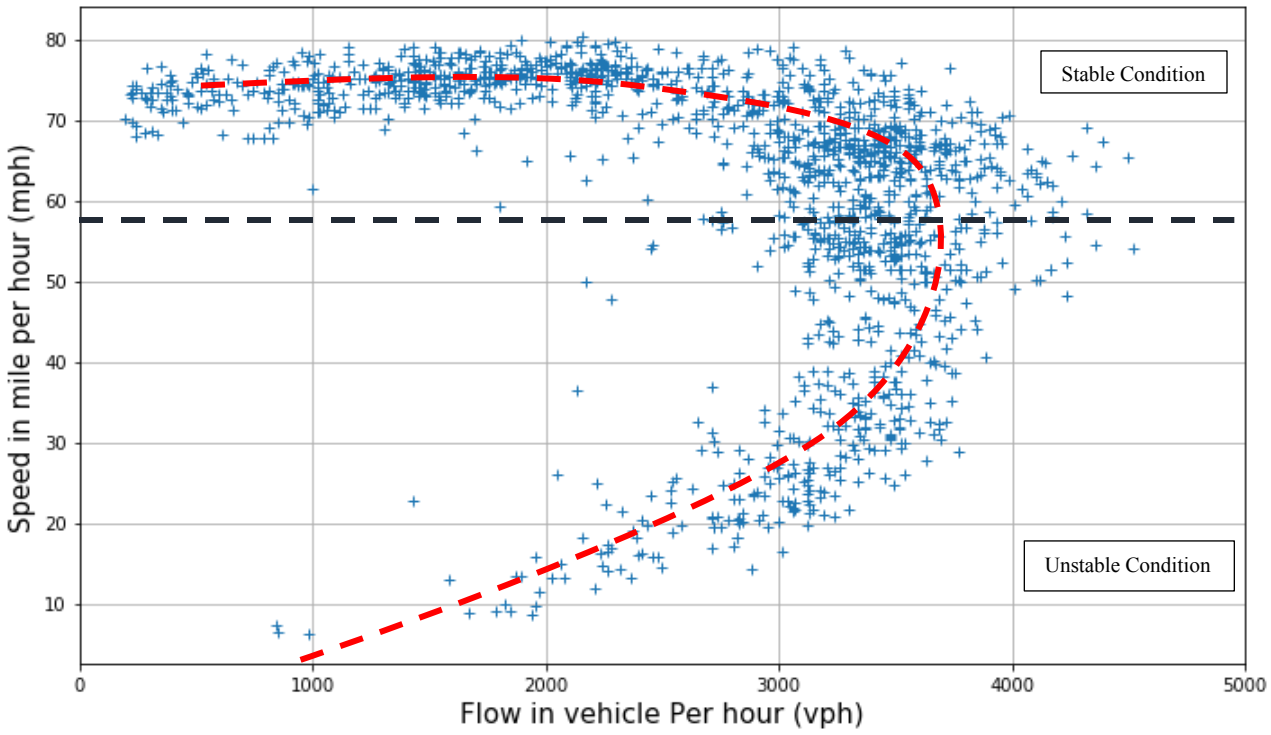

(a) Traffic Data for both Evacuation and Non-evacuation Condition (September 4, 2017 to September 9, 2017)

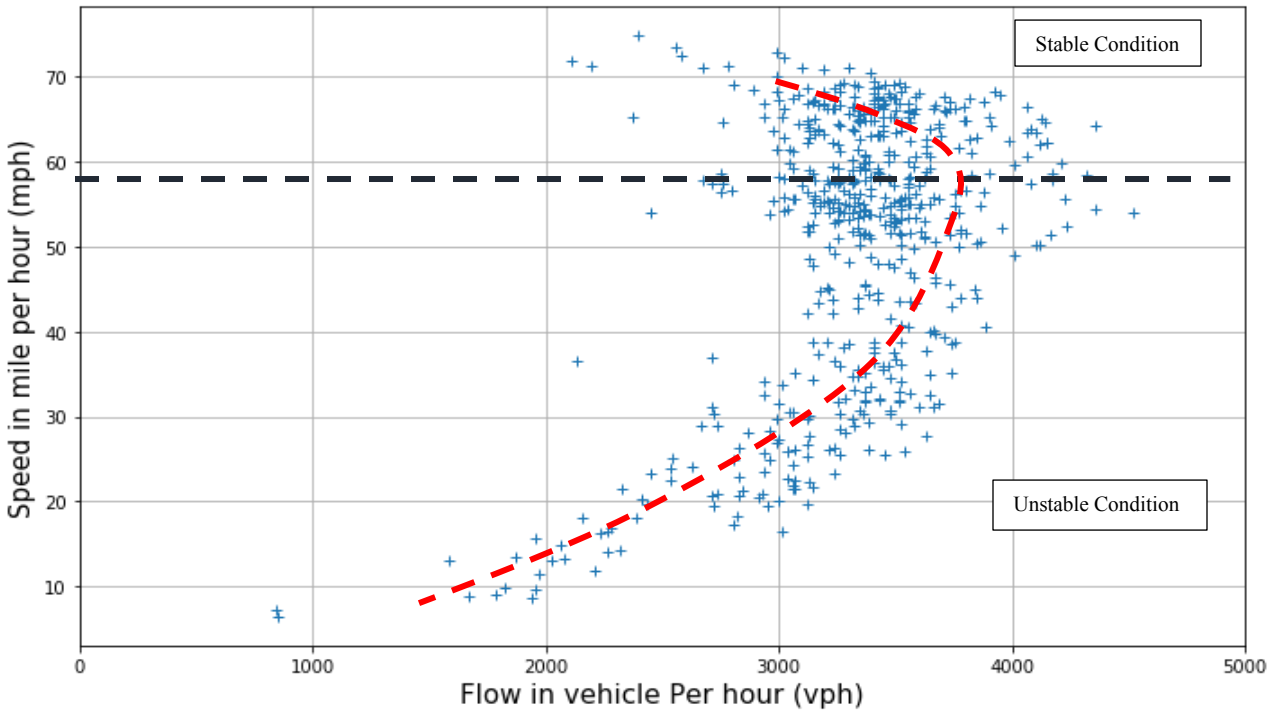

(b) Evacuation Traffic Condition ((September 07, 2017 to September 08, 2017)

Fig. 8. Traffic Speed vs. Flow Relationship for different Traffic Condition, the dashed dark line indicates optimal flow condition (for all three lane)

References

A Policy on Geometric Design of Highways and Streets, 6th ed, 2011. . American Association of State Highway and Transportation Officials. https://doi.org/265571500

Abdel-Aty, M., Uddin, N., Pande, A., 2005. Split Models for Predicting Multivehicle Crashes During High-Speed and Low-Speed Operating Conditions on Freeways. Transp. Res. Rec. J. Transp. Res. Board 1908, 51–58. https://doi.org/10.3141/1908-07

Abdel-aty, M., Uddin, N., Pande, A., Abdalla, M.F., Hsia, L., 2004. Predicting Freeway Crashes from Loop Detector Data by Matched Case-Control Logistic Regression 88–95.

Abdel-Aty, M., Wang, L., 2017. Implementation of Variable Speed Limits to Improve Safety of Congested Expressway Weaving Segments in Microsimulation. Transp. Res. Procedia 27, 577–584. https://doi.org/10.1016/j.trpro.2017.12.061

Abdel-Aty, M.A., Abdelwahab, H.T., 2003. Configuration Analysis of Two-Vehicle Rear-End Crashes. Transp. Res. Rec. J. Transp. Res. Board 1840, 140–147. https://doi.org/10.3141/1840-16

Aust, M.L., Engström, J., Viström, M., 2013. Effects of forward collision warning and repeated event exposure on emergency braking. Transp. Res. Part F Traffic Psychol. Behav. 18, 34–46. https://doi.org/10.1016/j.trf.2012.12.010

Bash, E., 2012. The GEH measure and quality of the highway assignment m, European Transport Conference. Glasgow, Scotland. https://doi.org/10.1017/CBO9781107415324.004

Bieker-Walz, L., Behrisch, M., Junghans, M., Gimm, K., 2017. Evaluation of car-following-models at controlled intersections. 31st Annu. Eur. Simul. Model. Conf. 2017, ESM 2017 238–243.

Bose, A., Ioannou, P., 2003. Mixed manual/semi-automated traffic: A macroscopic analysis. Transp. Res. Part C Emerg. Technol. 11, 439–462. https://doi.org/10.1016/j.trc.2002.04.001

Bueno, M., Fabrigoule, C., Ndiaye, D., Fort, A., 2014. Behavioural adaptation and effectiveness of a Forward Collision Warning System depending on a secondary cognitive task. Transp. Res. Part F Traffic Psychol. Behav. 24, 158–168. https://doi.org/10.1016/j.trf.2014.04.012

Cooper, D.F., Ferguson, N., 1976. Traffic studies at T-Junctions. 2. A conflict simulation Record. Traffic Eng. Control 17.

Dixit, V., Wolshon, B., 2014. Evacuation traffic dynamics. Transp. Res. Part C Emerg. Technol. 49, 114–125. https://doi.org/10.1016/j.trc.2014.10.014

Essa, M., Sayed, T., 2015. Transferability of calibrated microsimulation model parameters for safety assessment using simulated conflicts. Accid. Anal. Prev. 84, 41–53. https://doi.org/10.1016/j.aap.2015.08.005

Guo, Y., Essa, M., Sayed, T., Haque, M.M., Washington, S., 2019. A comparison between simulated and field-measured conflicts for safety assessment of signalized intersections in Australia. Transp. Res. Part C Emerg. Technol. 101, 96–110. https://doi.org/10.1016/j.trc.2019.02.009

Harigovindan, V.P., Babu, A. V., Jacob, L., 2014. Proportional fair resource allocation in vehicle-to-infrastructure networks for drive-thru Internet applications. Comput. Commun. 40, 33–50. https://doi.org/10.1016/j.comcom.2013.12.001

Hayward, J.C., 1972. Near-miss determination through use of a scale of danger. Highw. Res. Rec. 384, 22–34.

Jeffery Archer, 2005. Indicators for traffic safety assessment and prediction and their application in micro-simulation modelling: A study of urban and suburban intersections. KTH Royal Institute of Technology.

Jeong, E., Oh, C., Lee, S., 2017. Is vehicle automation enough to prevent crashes? Role of traffic operations in automated driving environments for traffic safety. Accid. Anal. Prev. 104, 115–124. https://doi.org/10.1016/j.aap.2017.05.002

Kamalanathsharma, R.K., Rakha, H.A., Zohdy, I.H., 2015. Survey on In-vehicle Technology Use: Results and Findings. Int. J. Transp. Sci. Technol. 4, 135–149. https://doi.org/10.1260/2046-0430.4.2.135

Kanagaraj, V., Asaithambi, G., Kumar, C.H.N., Srinivasan, K.K., Sivanandan, R., 2013. Evaluation of Different Vehicle Following Models Under Mixed Traffic Conditions. Procedia - Soc. Behav. Sci. 104, 390–401. https://doi.org/10.1016/j.sbspro.2013.11.132

Katrakazas, C., Quddus, M., Chen, W.H., 2018. A simulation study of predicting real-time conflict-prone traffic conditions. IEEE Trans. Intell. Transp. Syst. 19, 3196–3207. https://doi.org/10.1109/TITS.2017.2769158

Kesting, A., Treiber, M., Schönhof, M., Helbing, D., 2008. Adaptive cruise control design for active congestion avoidance. Transp. Res. Part C Emerg. Technol. 16, 668–683. https://doi.org/10.1016/j.trc.2007.12.004

Kim, J.-K., Wang, Y., Ulfarsson, G.F., 2007. Modeling the Probability of Freeway Rear-End Crash Occurrence. J. Transp. Eng. 133, 11–19. https://doi.org/10.1061/(asce)0733-947x(2007)133:1(11)

Kraus, S., 1998. Microscopic Modeling ofTraffic Flow: Investigation of Collision Free Vehicle Dynamics. Doctoral dissertation, Dt. Zentrum für Luft-und Raumfahrt eV, Abt. Unternehmensorganisation und-information.

Lee, J., Abdel-Aty, M., Wang, L., 2016. Utilizing Micro Simulation to Evaluate the Safety and Efficiency of the Expressway System.

Li, Y., Li, Z., Wang, H., Wang, W., Xing, L., 2017a. Evaluating the safety impact of adaptive cruise control in traffic oscillations on freeways. Accid. Anal. Prev. 104, 137–145. https://doi.org/10.1016/j.aap.2017.04.025

Li, Y., Wang, H., Wang, W., Liu, S., Xiang, Y., 2016. Reducing the risk of rear-end collisions with infrastructure-to-vehicle (I2V) integration of variable speed limit control and adaptive cruise control system. Traffic Inj. Prev. 17, 597–603. https://doi.org/10.1080/15389588.2015.1121384

Li, Y., Wang, H., Wang, W., Xing, L., Liu, S., Wei, X., 2017b. Evaluation of the impacts of cooperative adaptive cruise control on reducing rear-end collision risks on freeways. Accid. Anal. Prev. 98, 87–95. https://doi.org/10.1016/j.aap.2016.09.015

Li, Y., Xing, L., Wang, W., Wang, H., Dong, C., Liu, S., 2017c. Evaluating impacts of different longitudinal driver assistance systems on reducing multi-vehicle rear-end crashes during small-scale inclement weather. Accid. Anal. Prev. 107, 63–76. https://doi.org/10.1016/j.aap.2017.07.014

Liu, H., Kan, X. (David), Shladover, S.E., Lu, X.Y., Ferlis, R.E., 2018. Modeling impacts of Cooperative Adaptive Cruise Control on mixed traffic flow in multi-lane freeway facilities. Transp. Res. Part C Emerg. Technol. 95, 261–279. https://doi.org/10.1016/j.trc.2018.07.027

Marsden, G., McDonald, M., Brackstone, M., 2001. Towards an understanding of adaptive cruise control. Transp. Res. Part C Emerg. Technol. 9, 33–51. https://doi.org/10.1016/S0968-090X(00)00022-X

Martín de Diego, I., S. Siordia, O., Crespo, R., Conde, C., Cabello, E., 2013. Analysis of hands activity for automatic driving risk detection. Transp. Res. Part C Emerg. Technol. 26, 380–395. https://doi.org/10.1016/j.trc.2012.10.006

Milanés, V., Shladover, S.E., 2016. Handling Cut-In Vehicles in Strings of Cooperative Adaptive Cruise Control Vehicles. J. Intell. Transp. Syst. Technol. Planning, Oper. 20, 178–191. https://doi.org/10.1080/15472450.2015.1016023

Milanés, V., Shladover, S.E., 2014. Modeling cooperative and autonomous adaptive cruise control dynamic responses using experimental data. Transp. Res. Part C Emerg. Technol. 48, 285–300. https://doi.org/10.1016/j.trc.2014.09.001

Milanes, V., Shladover, S.E., Spring, J., Nowakowski, C., Kawazoe, H., Nakamura, M., 2014. Cooperative adaptive cruise control in real traffic situations. IEEE Trans. Intell. Transp. Syst. 15, 296–305. https://doi.org/10.1109/TITS.2013.2278494

Mintsis, E., 2018. Modelling, simulation and assessment of vehicle automations and automated vehicles' driver behaviour in mixed traffic 2018, 113.

Murray-Tuite, P., Wolshon, B., 2013. Evacuation transportation modeling: An overview of research, development, and practice. Transp. Res. Part C Emerg. Technol. 27, 25–45. https://doi.org/10.1016/j.trc.2012.11.005

Murray-Tuite, P., Wolshon, B., Matherly, D., 2017. Evacuation and Emergency Transportation: Techniques and Strategis for Systems Resilience. TR NEWS 311, 20.

National Research Council (U.S.). Transportation Research Board, 2010. HCM 2010: Highway Capacity Manual. Transportation Research Board, WASHINGTON, D.C.

Nezamuddin, N., Jiang, N., Zhang, T., Waller, S.T., 2011. Traffic operations and safety benefits of active traffic strategies on txdot freeways 7.

Porfyri, K.N., Mintsis, E., Mitsakis, E., 2018. Assessment of ACC and CACC systems using SUMO 2, 82–69. https://doi.org/10.29007/r343

Rahman, M.S., Abdel-Aty, M., 2018. Longitudinal safety evaluation of connected vehicles' platooning on expressways. Accid. Anal. Prev. 117, 381–391. https://doi.org/10.1016/j.aap.2017.12.012

Rahman, M.S., Abdel-Aty, M., Wang, L., Lee, J., 2018. Understanding the Highway Safety Benefits of Different Approaches of Connected Vehicles in Reduced Visibility Conditions. Transp. Res. Rec. https://doi.org/10.1177/0361198118776113

Rahman, R., Hasan, S., 2018. Short-Term Traffic Speed Prediction for Freeways during Hurricane Evacuation: A Deep Learning Approach. IEEE Conf. Intell. Transp. Syst. Proceedings, ITSC 2018-Novem, 1291–1296. https://doi.org/10.1109/ITSC.2018.8569443

Simulation of Urban Mobility: Simulation/Output/SSM Device [WWW Document], 2019. URL

https://sumo.dlr.de/docs/Simulation/Output/SSM_Device.html (accessed 5.7.19).

Simulation of Urban Mobility: Vehicle Type Parameter Defaults [WWW Document], 2019. URL https://sumo.dlr.de/docs/Vehicle_Type_Parameter_Defaults.html (accessed 5.7.19).

Talebpour, A., Mahmassani, H.S., 2016. Influence of connected and autonomous vehicles on traffic flow stability and throughput. Transp. Res. Part C Emerg. Technol. 71, 143–163. https://doi.org/10.1016/j.trc.2016.07.007

Tanishita, M., van Wee, B., 2017. Impact of vehicle speeds and changes in mean speeds on per vehicle-kilometer traffic accident rates in Japan. IATSS Res. 41, 107–112. https://doi.org/10.1016/j.iatssr.2016.09.003

Tapani, A., 2012. Vehicle trajectory effects of adaptive cruise control. J. Intell. Transp. Syst. Technol. Planning, Oper. 16, 36–44. https://doi.org/10.1080/15472450.2012.639641

Treiber, M., Kesting, A., 2013. Traffic Flow Dynamics chp 11 Car-Following Models based on Driving Strategies, in: Traffic Flow Dynamics. Springer, pp. 181--204.

Treiber, Martin, Kesting, A., 2013. Traffic Flow Dynamics, Traffic Flow Dynamics. Springer Berlin Heidelberg, Berlin, Heidelberg. https://doi.org/10.1007/978-3-642-32460-4

Van Der Horst, R., Hogema, J., 1993. Time-to-collision and collision avoidance systems. Proc. 6th Work. Int. 1–12.

van Nunen, E., Kwakkernaat, M.R.J.A.E., Ploeg, J., Netten, B.D., 2012. Cooperative Competition for Future Mobility. IEEE Trans. Intell. Transp. Syst. 13, 1018–1025. https://doi.org/10.1109/tits.2012.2200475

Wang, J., Rajamani, R., 2004. The impact of adaptive cruise control systems on highway safety and traffic flow. Proc. Inst. Mech. Eng. Part D J. Automob. Eng. 218, 111–130. https://doi.org/10.1243/095440704772913918

Wu, Y., Abdel-Aty, M., Lee, J., 2018. Crash risk analysis during fog conditions using real-time traffic data. Accid. Anal. Prev. 114, 4–11. https://doi.org/10.1016/j.aap.2017.05.004

Xiao, L., Wang, M., van Arem, B., 2017. Realistic Car-Following Models for Microscopic Simulation of Adaptive and Cooperative Adaptive Cruise Control Vehicles. Transp. Res. Rec. J. Transp. Res. Board 2623, 1–9. https://doi.org/10.3141/2623-01

Xu, C., Liu, P., Wang, W., Li, Z., 2012. Evaluation of the impacts of traffic states on crash risks on freeways. Accid. Anal. Prev. 47, 162–171. https://doi.org/10.1016/j.aap.2012.01.020

Yue, L., Abdel-Aty, M., Wu, Y., Wang, L., 2018. Assessment of the safety benefits of vehicles' advanced driver assistance, connectivity and low level automation systems. Accid. Anal. Prev. 117, 55–64. https://doi.org/10.1016/j.aap.2018.04.002

Zeeb, K., Buchner, A., Schrauf, M., 2015. What determines the take-over time? An integrated

model approach of driver take-over after automated driving. Accid. Anal. Prev. 78, 212–221. https://doi.org/10.1016/j.aap.2015.02.023

Zheng, Z., Ahn, S., Monsere, C.M., 2010. Impact of traffic oscillations on freeway crash occurrences. Accid. Anal. Prev. 42, 626–636. https://doi.org/10.1016/j.aap.2009.10.009